ground water

Environmental Isotopes as Indicators for Ground Water Recharge to Fractured Granite

by U.S. Ofterdinger[1], W. Balderer[2], S. Loew[2], and P. Renard[3]

Abstract

To assess the contribution of accumulated winter precipitation and glacial meltwater to the recharge of deep ground water flow systems in fracture crystalline rocks, measurements of environmental isotope ratios, hydrochemical composition, and in situ parameters of ground water were performed in a deep tunnel. The measurements demonstrate the significance of these ground water recharge components for deep ground water flow systems in fractured granites of a high alpine catchment in the Central Alps, Switzerland. Hydrochemical and in situ parameters, as well as $\delta^{18}O$ in ground water samples collected in the tunnel, show only small temporal variations. The precipitation record of $\delta^{18}O$ shows seasonal variations of ~14‰ and a decrease of 0.23‰ ± 0.03‰ per 100 m elevation gain. $\delta^{2}H$ and $\delta^{18}O$ in precipitation are well correlated and plot close to the meteoric water line, as well as $\delta^{2}H$ and $\delta^{18}O$ in ground water samples, reflecting the meteoric origin of the latter. The depletion of ^{18}O in ground water compared to ^{18}O content in precipitation during the ground water recharge period indicates significant contributions from accumulated depleted winter precipitation to ground water recharge. The hydrochemical composition of the encountered ground water, Na-Ca-HCO_3-SO_4(-F), reflects an evolution of the ground water along the flowpath through the granite body. Observed tritium concentrations in ground water range from 2.6 to 16.6 TU, with the lowest values associated with a local negative temperature anomaly and anomalous depleted ^{18}O in ground water. This demonstrates the effect of local ground water recharge from meltwater of submodern glacial ice. Such localized recharge from glaciated areas occurs along preferential flowpaths within the granite body that are mainly controlled by observed hydraulic active shear fractures and cataclastic faults.

Introduction

High alpine catchments in heterogeneous fractured crystalline rocks present a great challenge when assessing the large-scale ground water flow systems within these formations. Regional flow systems in mountainous terrain have been theoretically addressed by Tóth (1963, 1984), Forster and Smith (1988a, 1988b), and Zijl (l999), while the impact of fault zones on such systems was studied by López and Smith (1995). Among others, studies in crystalline massifs of Switzerland and France show the influence of the degree of fracturations and their orientation on preferential flowpaths on the massif scale (Lhomme et al. 1996; Pistre 1993). Crucial factors for understanding the nature of the flow systems are the analysis of the origin of encountered ground water and especially the recharge conditions in these topographically complex terrains. Systematic studies of the chemical composition of ground water encountered in crystalline formations of the Swiss Alps show how these parameters can assist in delineating the origin of the encountered waters (Dubois 1993). Recharge conditions in these high mountainous areas are strongly influenced by seasonal variations (Kattelmann and Elder 1991). Accumulated winter precipitation in the snowpack and meltwater from glaciated areas both contribute to ground water recharge (Martinec et al. 1982; Forster and Smith 1988a). The influence of the surface hydrology and, in particular, that of snowmelt and glaciation on shallow ground water systems has been investigated and a characteristic signature of this recharge source was shown in terms of environmental isotope content and

[1]URS Ireland Ltd., Iveagh Court, 6–8 Harcourt Rd., Dublin 2, Ireland; +353–1–4155100; fax +353–1–4155101; ulrich_ofterdinger@urscorp.com

[2]ETH Zurich, Engineering Geology, ETH-Hoenggerberg, CH–8093 Zurich, Switzerland

[3]University of Neuchâtel, Centre of Hydrogeology, 11 Rue Emile Argand, CH–2007 Neuchâtel, Switzerland

Received May 2002, accepted February 2004.

hydrodynamic response (Abbott et al. 2000; Flerchinger et al. 1992; Ward et al. 1999). However, these investigations are mainly restricted to shallow ground water systems in the decompressed zone of the basement rock (Cruchet 1985) with near surface weathering and stress relief.

To investigate the effects of the specific recharge conditions in high alpine regions on the deeper flow systems within fractured crystalline rocks, a high relief catchment (total area ~40 km^2) in the western Gotthard Massif was chosen for this study. Results from a hydrological model (PREVAV-ETH) applied to the research area provide estimates of spatially and temporally distributed ground water recharge rates (Vitvar and Gurtz 1999), indicating high recharge rates in the glaciated areas during ablation periods. Even though only a small percentage (~14.6%) of the total catchment is glaciated, significant effects on the ground water flow regime are anticipated, particularly regarding the flow to a deep and unlined tunnel (Bedretto Tunnel), which partly passes beneath the research area and its glaciated regions. This tunnel was used for direct subsurface observations and monitoring of ground water flow and sampling. Analysis of the hydrochemical composition, as well as the environmental isotope content, was used to establish the relationship between surface waters, spring discharges, and deeper ground water. Interpretation of the data was furthermore based on the analysis of the structural anisotropy and heterogeneity of the host rock due to fracturation and faulting.

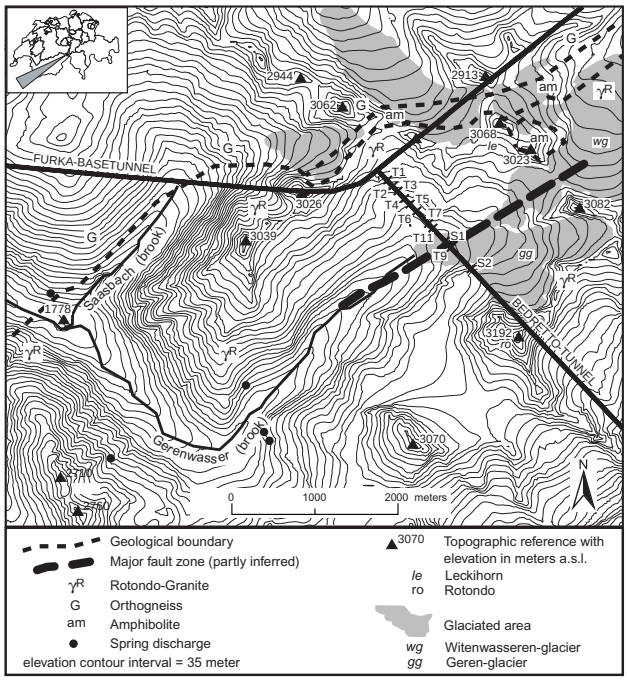

Figure 1. Enlarged plan view of the research area. Indicated are the projected tunnel traces together with the location of the subsurface observation points, geological boundaries. and the trace of the major fault zone intersecting the Bedretto Tunnel. Locations of spring discharges and glaciated areas are also marked.

Geological Setting

The research area is situated in the western Gotthard Massif of the Swiss Alps. Geologically, it consists mainly of the late Hercynian Rotondo Granite, ~220 Ma (Jäger and Niggli 1964) and orthogneiss of early Palaeozoic age, ~420 Ma (Arnold 1970). Topographic elevation of the granite body ranges from 1800 to 3200 m a.s.l. (Figure 1).

On the northern margin of the study area, the Furka Basetunnel passes through the granite body at an elevation of ~1490 m a.s.l. An abandoned and unlined support segment to this basetunnel, the Bedretto Tunnel is furthermore passing through the granite body in a northwest-southeast direction. Due to the partial collapse of the tunnel, only the northern ~1.5 km are still accessible. Figure 1 shows that this latter tunnel segment is also passing beneath glaciated areas of the study domain. It offers the opportunity for direct subsurface observations, and was used for sampling of ground water, monitoring of discharges, and in situ parameters. The granite body shows varying degrees of fracturation and faulting throughout the research domain, changing both in lateral and vertical directions. Data on fracture orientation and fracture frequency were gathered by means of scanline surveys (Priest 1993) on surface outcrops and along the unlined tunnel profile of the Bedretto Tunnel. From this data, four major fracture sets can be deduced (Table 1), where, especially, sets 1 and 2 are dominant at the terrain surface. The northwest-southeast striking fracture sets (sets 3 and 4) are more abundant along the tunnel profile and are believed to be influenced by the tunnel construction, i.e., induced or reactivated by local stress amplifications.

In addition to these steeply dipping sets, further shallow dipping fractures can be identified at the terrain surface. These latter fractures generally strike subparallel to the valleys with dip directions toward the valley bottom, most probably representing quaternary stress release joints. Occasionally, concentrical jointing can also be observed within the granite at the terrain surface. In addition to the fracturation, steeply dipping fault zones can be identified as important larger features, both at the surface and along the tunnel profile. They are mostly orientated subparallel or at acute angles to the general trend of the alpine structures of the Gotthard Massif (east northeast–west southwest). One of the major fault zones intersecting the Bedretto Tunnel is indicated in Figure 1. Both preferred orientations of fracturation (strike east northeast–west southwest) and, on a larger scale, the orientation of fault zones cause a significant structural anisotropy within the granite body.

Table 1
Mean Orientation of Fracture Sets and Corresponding Mean Normal Fracture Frequency λ (Priest 1993) from Surface and Tunnel Outcrops

Set Number	Mean Orientation (strike/dip)	$\lambda_{surface}$ (m^{-1})	λ_{tunnel} (m^{-1})
1	049/75 SE	2.1	0.5
2	080/83 SE	1.5	0.2
3	140/86 SW	0.7	2.6
4	170/79 SW	0.04	0.3

Hydrochemistry

Samples of the encountered ground water were collected from spring discharges at the terrain surface of the granite body, as well as from inflows to the Bedretto Tunnel. Their major ionic composition was analyzed by ion-exchange liquid chromatography, while parameters such as pH, temperature, conductivity, alkalinity, and oxygen content were measured in situ during sampling with electronic probes or field titration, respectively. Saturation indices (SI = log IAP/K_T) for several minerals where calculated with WATEQ4F (Ball and Nordstrom1992).

Spring Discharges

Few spring discharges from the granite body can be identified in the research area. They are mostly associated with zones of denser fracturation with northeast-southwest striking, steeply dipping fractures (Figure 1). Table 2 gives an overview of the average in situ parameters measured at these spring discharges during three successive summer field campaigns (1997–1999). In terms of decreasing mEq% of cations and anions, respectively, the encountered waters are characterized as dilute, slightly alkaline Ca-Na-HCO_3(-SO_4) waters. Their mean Ca/Na ratio, deduced from mEq/L concentrations, lies at 2.58 (σ = 0.9). All encountered waters are undersaturated with regard to calcium-bearing minerals such as calcite or sulfate minerals such as gypsum or anhydrite (mean value for $SI_{Calcite}$ = 3.417, σ = 0.122; SI_{Gypsum} = –4.793, σ = 0.151; $SI_{Anhydrite}$ = –4.541, σ = 0.151). Spring discharge from the northern orthogneiss shows a different hydrochemical composition and can be characterized as Ca-HCO_3-(SO_4) waters with a mean Ca/Na ratio of 8.93 (σ = 1.26). Mean in situ parameters are stated in Table 2. Compared to the spring waters encountered from the granite body, the discharge from the orthogneiss is less, but still undersaturated with regard to calcium-bearing minerals or sulfate minerals (mean value for $SI_{Calcite}$ = –1.756, σ = 0.276; SI_{Gypsum} = –3.691, σ = 0.046; $SI_{Anhydrite}$ = –3.948, σ = 0.045).

Tunnel Inflows

Along the ~1.5 km accessible section of the unlined Bedretto Tunnel, 11 tunnel inflows were monitored and sampled (Figure 1). Hydrochemical sampling was carried out from September 1998 until November 1999 (15 months) on a monthly or bimonthly basis, while in situ parameters were measured from September 1998 until August 2000. Ground water samples were collected directly at the rock-face from discrete features such as fractures and fault zones. Measurements of discharge rates at the individual sampling locations were carried out manually with calibrated vessels. For measurements of integral inflow rates along particular tunnel sections, depth-integrated flow velocity measurements with an anemometer were carried out along cross sections in the basal drain of the tunnel, which cumulatively captures the tunnel inflows. Discharge was then calculated according to ISO748:1997(E) (ISO 1997). At the specific observation points S1 and S2 (Figure 1), triangular-notch thin-plate weirs, in accordance with ISO1438/1:1980(E) (ISO 1980), equipped with float level gauges, were installed for continuous measurement of the collected discharge at these locations. Measurements were recorded from January 1999 until August 2000. However, the records prior to mid-June 1999 were partly obscured by technical problems and damages caused by rock bursts in the gallery. Discharge rates were calculated from the records applying the Kindsvater-Shen formula (ISO 1980).

Table 2
Mean In Situ Parameters

Location	Q (L/min)	Temperature (°C)	κ (µS/cm)	pH	TDS (meq/L)	O_2 (mg/L)
T1	0.6 (0.11)	19.3 (0.2)	83.1 (1.4)	8.9 (0.2)	1.64 (0.07)	2.7 (0.2)
T2	26.9 (1.22)	19.7 (0.1)	88.1 (1.4)	9.0 (0.2)	1.73 (0.07)	2.3 (0.2)
T3	0.6 (0.03)	19.9 (0.2)	71.8 (1.6)	9.1 (0.1)	1.37 (0.10)	3.0 (0.1)
T4	0.8 (0.07)	19.3 (0.2)	94.0 (1.6)	8.9 (0.1)	1.89 (0.12)	1.1 (0.3)
T5	2.1 (0.23)	19.7 (0.1)	89.1 (1.5)	9.1 (0.1)	1.71 (0.10)	2.4 (0.3)
T6	1.1 (0.10)	19.6 (0.1)	89.4 (1.4)	9.1 (0.1)	1.74 (0.05)	1.9 (0.2)
T7	6.6 (0.85)	19.0 (0.1)	104.0 (1.7)	9.1 (0.1)	1.99 (0.14)	1.8 (0.3)
T9	10.3 (0.65)	15.4 (0.27)	91.5 (1.9)	9.2 (0.1)	1.76 (0.12)	1.2 (0.2)
T11	3.0 (0.27)	19.6 (0.05)	115.1 (1.7)	9.3 (0.1)	2.14 (0.14)	0.3 (0.1)
S1	18.4 (0.47)	17.7 (0.1)	105.5 (2.2)	9.2 (0.1)	2.10 (0.10)	2.0 (0.2)
S2	30.5 (1.91)	18.9 (0.04)	79.2 (1.4)	8.9 (0.1)	1.54 (0.10)	2.9 (0.3)
Q (γ_R)		7.9 (1.6)	16.0 (1.5)	7.2 (0.3)	0.35 (0.05)	8.1 (0.8)
Q (G)		6.5 (0.6)	64.7 (2.5)	7.3 (0.3)	1.27 (0.05)	6.7 (0.2)

Mean in situ parameters (discharge Q, temperature, conductivity **κ**, pH, total dissolved solids [TDS] and dissolved oxygen [O_2] at individual sampling locations along the tunnel, as well as mean in situ parameters for spring discharges from the Rotondo Granite (γ_R) and the neighboring orthogneis (G) (Figure 1). Standard deviation in parentheses as indicator for variability over time.

Similar to the surface observations, inflows are mainly associated with northeast-southwest striking fractures and/or fault zones. This indicates that the observed dominant fracture orientations not only cause a strong structural anisotropy within the granite body, but are furthermore causing a hydraulic anisotropy and heterogeneity favoring preferential flow in the plane of these features. The observation points T9 and S1 are associated with a major steeply dipping fault zone, striking ~75° (Figure 1). This ~120 m wide zone consists of several discrete cataclastic faults, partly with clay mineral infilling (gouge), and neighboring zones of dense fracturation. Along this zone, the most significant inflows to the tunnel occur. Discrete inflows in this zone are abundant, but often obscured by tunnel support systems.

The discharge rates at the individual sampling locations along the tunnel profile range from drop-inflows with mean rates of 0.56 to 0.85 L/min to more significant inflows with mean discharge rates up to 33.8 L/min. Even though small variations from the mean value of discharge

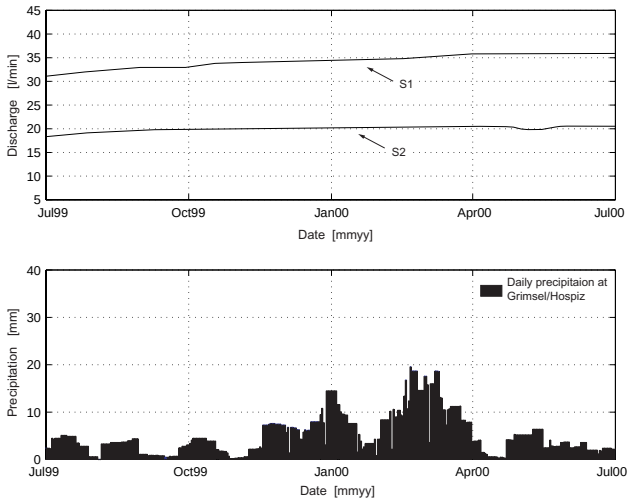

Figure 2. Record of automated discharge measurements S1 and S2 in the Bedretto Tunnel together with daily precipitation recorded at the meteorological station Grimsel/Hospiz (1980 m a.s.l).

over time can be observed in the manual measurements at these locations, the automated stations at S1 and S2 show no significant small-scale temporal variations of discharge. Figure 2 depicts the discharge rates at these stations for the recent period of 1 yr together with the daily precipitation at the meteorological station Grimsel/Hospiz (1980 m a.s.l.), located in the northern vicinity of the research area. Both discharge records show a steadily increasing trend, but no direct response to recent precipitation in this period. Fluctuations are only minor with respect to the registration resolution of the gauges at S1 and S2 (0.7 and 0.9 L/min, respectively). However, the small, but consistent, increase of discharge might be linked to the large-scale annual fluctuations of total precipitation. Figure 3 shows the annual precipitation at Grimsel/Hospiz for the period from July 1990 to July 2000. It is apparent that the past 3 yr have been characterized by high total precipitation and, thus, the discharge rates at the stations might be showing a delayed response to these long-term variations in precipitation.

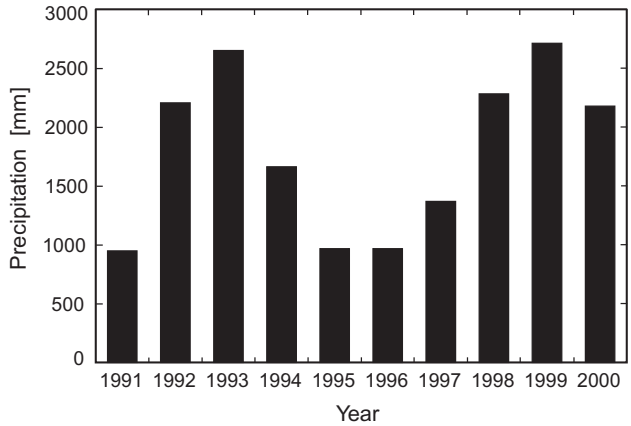

Figure 3. Record of annual precipitation (1990–2000 summed for period July–July) at the meteorological station Grimsel/Hospiz (1980 m a.s.l.).

Total discharge along the whole ~1.5 km tunnel section amounts to a mean value of 890 L/min. The variations over time around this average value are again small (σ = 18 L/min) and are within the range of the potential measurement error (± 24 L/min).

Table 2 gives an overview of the manually measured in situ parameters for the individual observation points along the Bedretto Tunnel. The temperature measurements show only little variation over time at the individual sampling locations and along the tunnel profile, except for a significant negative temperature anomaly at locations T9 and, to a lesser degree, S1. Temporal variability at T9 is the highest (σ = 0.27°C). These two sampling locations are associated with the large fault zone encountered along the gallery (Figure 1), where ground water inflow to the tunnel occurs at high discharge rates (along the whole fault zone section ~450 L/min). Figure 4 illustrates this anomaly below the glaciated area and indicates the potential contribution of cold glacial waters to the ground water recharge.

The hydrochemical composition of the ground water encountered along the tunnel profile can mainly be described as dilute, moderately alkaline (pH 8.9 to 9.3) (Table 2) Na-Ca-HCO_3-SO_4(-F) waters with a mean Ca/Na ratio of 0.64 (σ = 0.21, deduced from mEq/L concentrations).

Saturation indices show undersaturation with regard to calcite or sulfate minerals as well as for fluorite for all samples taken from the tunnel inflows (mean value for $SI_{Calcite}$ = –0.184, σ = 0.051; SI_{Gypsum} = –3.284, σ = 0.159; $SI_{Anhydrite}$ = –3.535, σ = 0.156; $SI_{Fluorite}$ = –0.729, σ = 0.205). These waters have most probably evolved from the ground water composition as measured at the surface discharges mainly through the process of feldspar (plagioclase) hydrolysis along the flowpaths through the granite body. Petrographic studies of the Rotondo Granite (Hafner 1958) state a composition of the rock matrix of 25% to 35% quartz, 20% to 40% potassium feldspar, 20% to 35% albite, 2% to 7% anorthite, and 5% to 10% biotite with minor amounts of garnet, chlorite, epidote, and apatite. Local significant deposits of pyrite have been reported during the tunnel construction. During silicate weathering, sodium is released from the albite-rich granite. This process results in an alkalinity increase and calcium is most probably lost to the solid phase by ion-exchange processes on clay minerals contained in fillings and linings of fractures and/or fault zones. Precipitation of calcite is unlikely to occur as both spring samples and tunnel inflows are undersaturated with respect to calcite.

At the northern end of the Bedretto Tunnel, Ca-Na-HCO_3-SO_4(-F) waters with a mean Ca/Na ratio of 1.19 (σ = 0.07) are encountered. Several factors contribute to this changed Ca/Na ratio. Hafner (1958) reports a decreasing albite content within the granite composition toward the margins of the intrusive body. Therefore, these waters close to the northern boundary of the granite body may reflect this changing geochemical composition of the host rock. Additionally, the degree of fracturation and especially the number of large fault zones with significant clay infilling (gouge) is smaller in this part of the tunnel. Less abundance of these features would imply less potential for ion-exchange with clay minerals to remove calcium from

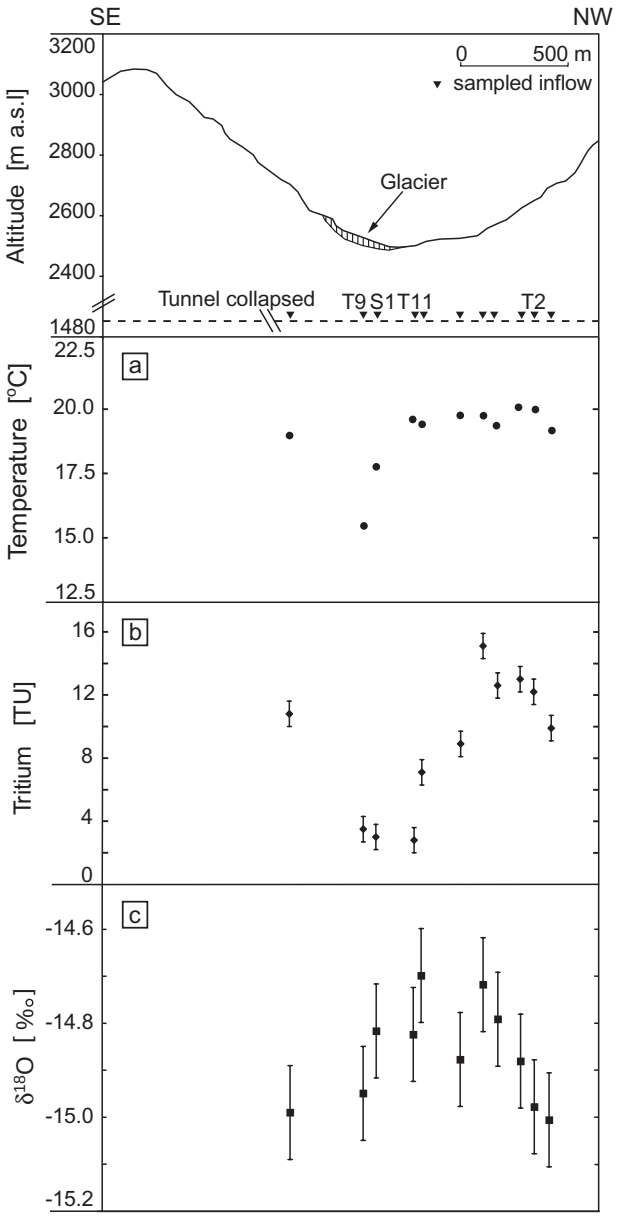

Figure 4. Cross section along the profile of the Bedretto Tunnel with locations of sampled inflows: (a) mean temperature, (b) mean tritium concentration, and (c) mean $\delta^{18}O$ content. Analytical error is indicated.

solution. Variations in the relative abundance of calcite within the granite body may also influence the range of observed Ca/Na ratio. Finally, influences from potentially calcium-richer ground waters originating in the neighboring orthogneiss and, in particular, in the amphibolite wedges within the gneiss (Figure 1) are other potential calcium sources as indicated by the analysis of spring discharges. Water from the amphibolite wedges could not be sampled; however, studies in the central Swiss Alps show that similar calcium-rich compositions can be expected to originate from the amphibolites (Marechal 1998). Because of the observed strong anisotropy of the gneiss, with steeply dipping schistosities, mainly aligned subparallel to the main orientation of the Gotthard Massif (east northeast–west southwest), a pronounced hydraulic anisotropy within these rocks seems plausible. This would imply preferential flowpaths along the strike of the schistosity planes and, together with the preferred orientation of observed hydraulic active fractures and fault zones within the granite body (east northeast–west southwest), potential contribution from these neighboring formations would most probably originate in the northeast direction of the granite body (Leckihorn area) (Figure 1).

Environmental Isotopes

To investigate potential sources of ground water recharge and flowpaths, as well as the age of the encountered waters, the contents in environmental isotopes of water samples from tunnel inflows were measured, i.e., contents of ^{18}O, ^{2}H, and tritium (^{3}H). Additionally, ^{18}O and ^{2}H content in precipitation were analyzed. ^{18}O and ^{2}H content, the latter after zinc reduction to H_2, in ground water and precipitation samples were determined by isotope ratio mass spectrometry. Tritium values of ground water samples were measured by means of an enriched liquid scintillation counter. Isotope composition is reported as d value of the heavy isotope = $(R_{Sample}/R_{Standard} - 1) \times 1000$ in units of ‰, where R = (heavy isotope/light isotope). Analytical errors in the previous $\delta^{18}O$ and $\delta^{2}H$ determination are ± 0.1‰. Tritium determinations are associated with an error of ± 0.8 TU (all expressed as 2σ).

The conventional standard for $\delta^{2}H$ and $\delta^{18}O$ values is Vienna Standard Mean Ocean Water. Tritium values (^{3}H) are reported as absolute concentrations in TU (1 TU corresponds to 1 tritium atom per 10^{18} hydrogen atoms or 0.118 Bq/L).

All isotope measurements were carried out at the GSF Institute of Hydrology in Neuherberg, Germany.

Tritium

For the analysis of the tritium content of the tunnel inflows, two sampling series were carried out and analyzed (December 1998 and March 1999). Differences in the tritium content at the individual sampling points between the two series do not exceed the accuracy of the measurement of ± 0.8 TU. The mean tritium concentrations observed at the sampling points along the tunnel profile (Figure 4) show values of 7.1 to 15.1 TU at the northwestern end of the tunnel. Values of 2.8 to 3.5 TU are observed toward the southeastern end of the profile below the glacier. At the southeastern end, the mean tritium content lies at 10.8 TU.

Qualitatively, for continental regions, tritium values of 5 to 15 TU are attributed to recent recharge (< 5 to 10 yr) while tritium contents of 0.8 to ~4 TU would represent a mixture between submodern (recharged prior to 1952) and recent recharge (Clark and Fritz 1997). Two possible scenarios might elucidate the presence of the low tritium values and the origin of the submodern component. The sampling sites showing these low tritium concentrations (T9, T11, and S1) are situated below the valley bottom and might be influenced by upwelling of old ground water from within the granite body. A plot of tritium content vs. sodium content (Figure 5) shows the negative correlation of tritium values with sodium content. This correlation is typically observed with the presence of older ground water components characterized by higher mineralization, i.e., sodium content. However, the sodium concentration of the low tritium samples is still small (< 0.7 meq/L). Other

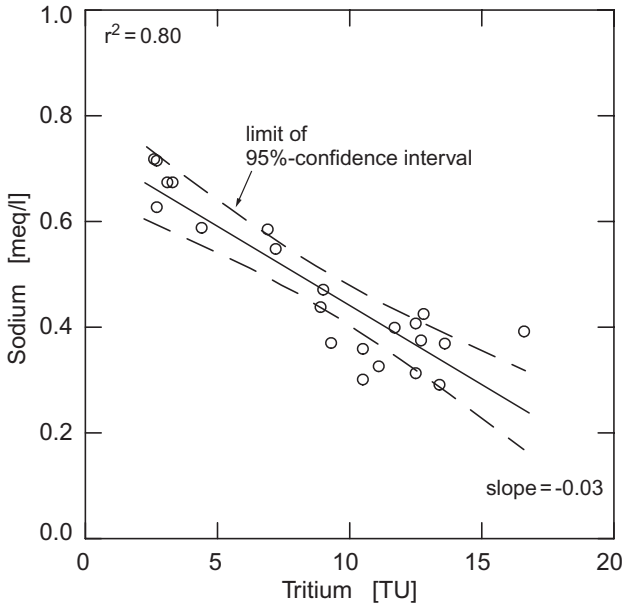

Figure 5. Plot of tritium vs. sodium content for samples from the Bedretto Tunnel.

studies in the central Swiss Alps show that for a causal relationship between sodium and tritium content with respect to a source of submodern ground water, sodium concentrations of at least > 1 meq/L are common (Marechal 1998). With regard to the petrographic analysis of the Rotondo Granite (Hafner 1958), the resulting correlation between low tritium values and small, but increased, sodium concentrations might merely be caused by coincidence with the observed spatial variation of albite content of the rock and, thus, the increased availability of sodium to go into solution away from the margins of the granite body. As the tunnel profile represents a transect from the margin of the body toward its center, this trend is reproduced in the water composition sampled at the specific locations.

Another scenario with regard to the influence of the glaciated areas above the observed inflows to the tunnel is also plausible. Meltwater from the glaciated areas is derived from a distinct reservoir, which preferentially accumulates winter precipitation with low tritium contents according to the observed seasonal variation in precipitation. However, the observed mean tritium concentrations in recent winter precipitation range from 8.4 to 15.8 TU (observations during the 1990s at meteorological stations Guttannen, Grimsel, and Meiringen in the northern vicinity of the research area). Therefore, ground water infiltration from this accumulated recent winter precipitation can only explain the observed data with lower values down to 2.8 TU, if the residence time of this water is assumed to exceed the half-life cycle of tritium (12.43 yr).

Another variant of this latter scenario is regarded to be most plausible. Assuming that not only recent accumulated winter precipitation with seasonal low tritium concentrations contributes to the ground water recharge, but also meltwater from old submodern glacial ice, a source of ground water recharge is present, which can explain the measured low tritium content. This source is tapped by the large fault zone associated with the observation points T9 and S1. On a plan view projection (Figure 1), it can be shown that the inferred trace of this structure passes beneath a large portion of the glaciated region that reaches up to altitudes of 3000 m a.s.l. Ground water recharged along the strike of this structure is anticipated to move by topography-driven flow and enhanced by the drainage to the subsurface gallery along this preferential flowpath toward the tunnel, thereby preserving the characteristic low tritium values of recharge from the glacial meltwater of the subglacial drainage system (Tranter et al. 1996). A similar influence of meltwater from tritium-free glacial ice on the overall tritium content of glacial discharge is also reported by Ambach et al. (1971) and, for the Grimsel area in the northern vicinity of the study area, by Keppler (1996).

The tritium values of 7.1 to 15.1 TU are in the range of the tritium concentrations in recent winter precipitation. For comparison, the tritium concentrations from recent summer precipitation are generally higher and range from 14.7 to 25.3 TU (observations during the 1990s at the meteorological stations Guttannen, Grimsel, and Meiringen in the northern vicinity of the research area). Thus, the observed tritium contents reflect the selectivity (Gat 1981) of ground water recharge mainly from recent accumulated winter precipitation. Snow cover in the study area is generally substantial and apart from the high availability of snow meltwater during the melting period; Rodhe (1998) describes the meltwater input to ground water recharge as very efficient. The snow temperature cannot exceed 0°C even if the atmosphere may be warm (and moist). Warm air will therefore give a small or negative vapor pressure difference between snow and the atmosphere and, thus, a small or negative evaporation (i.e., condensation). Furthermore, evaporation from water under the snowpack is negligible due to low temperatures and lack of turbulent exchange with the atmosphere.

The spread of the encountered tritium data can be attributed to varying flow velocities (reflected by the different tritium contents) within separate hydraulic features such as fractures and small-scale faults. In this sense, the ground water system might be viewed as an assemblage of discrete water parcels that move along defined flowpaths (Gat 1981). Similar observations were made by Fontes et al. (1978) in a comprehensive study in the Mont-Blanc Tunnel, where rapid recharge was indicated by the tritium data with flow velocities of ≥ 150 m/yr.

$^{2}H/^{18}O$ in Precipitation, Glacial Meltwater, and Ground Water

As a further means to evaluate the ground water recharge conditions in the study area, ^{2}H and ^{18}O contents in ground waters samples were analyzed in comparison to $d^{2}H$ and $\delta^{18}O$ values in precipitation and glacial meltwater. Qualitative observations were reproduced through a simple mathematical transport model using a convolution/lumped-parameter approach (Maloszewski and Zuber 1996, 1998) to investigate recharge conditions and, in particular, the contribution of glacial meltwater to the flow system. In this approach, an observed output function, e.g., $\delta^{18}O$ content over time in the ground water, is related to an observed input function, e.g., $\delta^{18}O$ content over time in precipitation, by the convolution integral. The type of transport model is chosen by defining a transit time distribution function and

parameterizing this latter function in order to calibrate the theoretical output of the convolution integral to the observed $\delta^{18}O$ record.

$^{2}H/^{18}O$ in Precipitation

Data on the $\delta^{18}O$ and $d^{2}H$ content of precipitation were obtained from three meteorological stations in Haslital in the north of the study area (Guttannen, Meiringen, and Grimsel/Hospiz 1970–1999) and from five additional stations in the eastern, western, and southern vicinity of the research area (Gütsch, Andermatt, Oberwald, Binn, and Robiei 1998–1999). These stations were chosen to cover the trajectories of potential precipitation to the study area. From this data, the local meteoric water line for the study area was derived following

$$\delta^{2}H = (7.65 \pm 0.05) \times \delta^{18}O + (4.7 \pm 0.77) \quad (1)$$

Figure 6 depicts this local meteoric water line and indicates its relationship to the meteoric water line defined by Craig (1961) as the locus of the isotope composition of worldwide fresh water sources. From the same given dataset, the $\delta^{18}O$ altitude (z) relationship was derived as

$$\delta^{18}O = (-0.0023 \pm 0.0003) \times z - (9.4 \pm 0.5) \quad (2)$$

This calculated $\delta^{18}O$ altitude correlation is in good agreement with published data (Pearson et al. 1991) giving a correlation for the northern central Swiss Alps of (Figure 7)

$$\delta^{18}O = (-0.0021 \pm 0.0006) \times z - (10.6 \pm 0.7) \quad (3)$$

The $\delta^{2}H$ altitude (z) relationship was derived as

$$\delta^{2}H = (-0.0146 \pm 0.0025) \times z - (71.46 \pm 3.86) \quad (4)$$

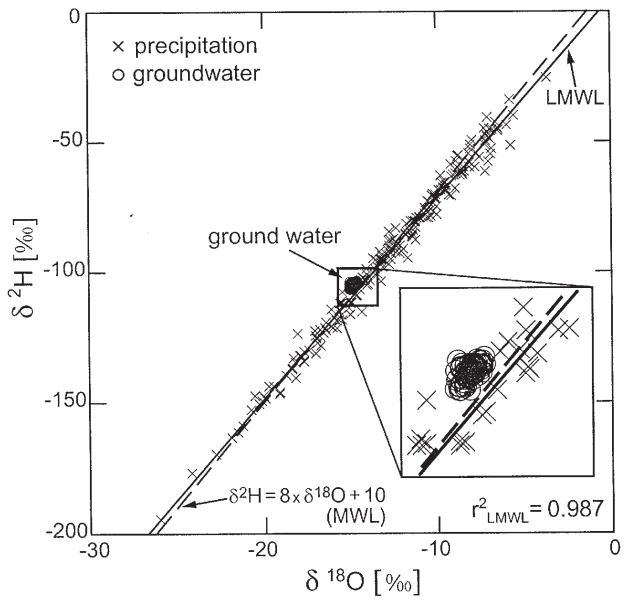

Figure 6. Local meteoric water line based on $\delta^{2}H/\delta^{18}O$ data from meteorological stations together with the meteoric water line as defined by Craig (1961). Indicated are also $\delta^{2}H/\delta^{18}O$ data from ground water samples collected in the Bedretto Tunnel.

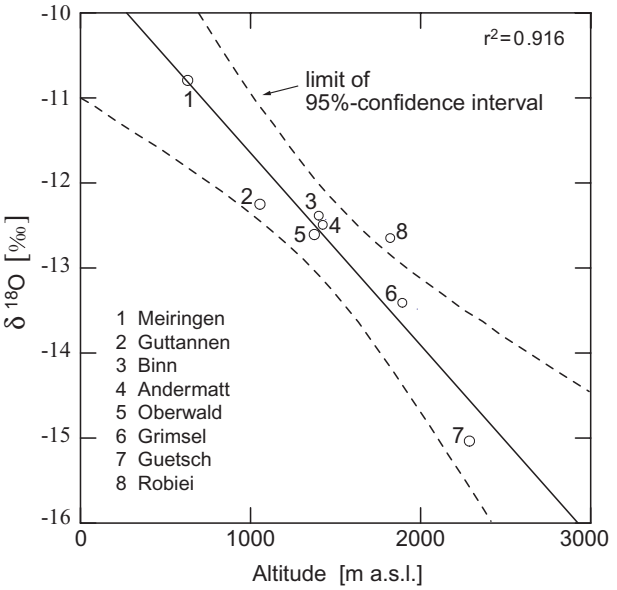

Figure 7. Relationship between altitude and mean annual $\delta^{18}O$ content in precipitation at meteorological stations near the research area.

The mean annual deuterium excess $d = \delta^{2}H - 8 \times \delta^{18}O$ in precipitation at the aforementioned meteorological stations ranges from 8.3‰ at Oberwald in the northern vicinity of the study area to 13.3‰ at Robiei in the south of the study area. Subtle seasonal variations in d can be observed, with deuterium excess values during the summer of 7.2‰ to 12.1‰ and during winter of 9‰ to 14.2‰, respectively. In the latter monthly maxima, up to 21‰ are observed. A general explanation for increased d values in winter precipitation lies in the type of precipitation during this period. Solid precipitation such as snow during the wintertime shows higher d values due to nonequilibrium condensation during the growth of the ice particles (Gat 2000; Jouzel and Merlivat 1984). Additionally, Schotterer et al. (1995) report that winter precipitation in the Alps originating from the Mediterranean Sea often shows increased d values.

$^{2}H/^{18}O$ in Glacial Meltwater

Glacial meltwater is characterized by a complex signal owing to varying fractions of snow- and icemelt contributing to the overall meltwater composition throughout the melting period. Furthermore, firnification of the accumulated snow cover, percolating meltwater, and liquid precipitation through the glacial body, sublimation and condensation, as well as melting and recrystallization, cause additional fractionations in the $\delta^{18}O$ of the ice and snow (Stichler and Schotterer 2000). Unfortunately, in the scope of this study, no sufficient data were available to clearly constrain these relationships. To investigate the significance of the contribution of glacial meltwater to ground water recharge, a strong simplification was made for the purpose of the succeeding mathematical model (Maloszewski and Zuber 1996) of $\delta^{18}O$ values.

Glacial meltwater is regarded as a combination of snow- and icemelt. At the onset of the ablation period, the contribution from snowmelt dominates while, at later times, melting of glacial ice becomes increasingly important

(Malard et al. 1999). As each of these two components can be considered as dominant for an equally long time during the total ablation period, the overall $\delta^{18}O$ concentration of glacial meltwater ($c\beta$) was derived from the arithmetic mean of $\delta^{18}O$ values in snow and glacial ice, respectively ($c\beta_{snow}$ and $c\beta_{ice}$). From balance equations, Ambach et al. (1971) show that the fraction of ice meltwater in total glacial discharge may even reach up to 60%. The $\delta^{18}O$ concentration of the snowmelt ($c\beta_{snow}$) was approximated from the mean annual value of winter precipitation (1970–1999) extrapolated to the mean altitude of the glacier. Values for the concentration in the glacial ice ($c\beta_{ice}$) were measured in five ice samples taken from the glacier, with $\delta^{18}O$ values ranging from –13.38‰ to –13.81‰ and d^2H values varying between –88.3‰ and –101.1‰, respectively. These few ice samples cannot be regarded as representative for the heterogeneous and complex signal originating from the glacial ice (Stichler and Schotterer 2000). Rather, it should be considered as an estimate for the potential contribution of glacial ice to the overall glacial melt component. The calculated estimate for the $\delta^{18}O$ concentration in the glacial meltwater amounts to $c\beta$ = –16.2‰.

$^2H/^{18}O$ in Ground Water

Ground water samples for ^2H and ^{18}O determination were collected on a monthly or bimonthly basis for a period of 1 yr (September 1998 until September 1999) along the ~1.5 km accessible section of the unlined Bedretto Tunnel. Eleven locations along the tunnel profile were sampled (Figure 1). The $\delta^{18}O$ values observed in the tunnel show only small variations. The meteoric origin of the ground water is shown by its alignment to the global meteoric water line (Figure 6). Figure 4 shows the mean $\delta^{18}O$ values measured at the individual sampling points along the tunnel profile. Mean deuterium excess *d* of the sampled ground water range from 13.3‰ to 14.5‰. Compared to the *d* values in recent precipitation at the meteorological stations, this may indicate a significant contribution of accumulated winter precipitation with relative higher *d* values to ground water recharge.

Generally, encountered ^{18}O values seem to reproduce the altitude effect, i.e., increase of overburden implies potentially higher recharge altitudes implying depleted ^{18}O in precipitation. From Equations 2 and 4, estimated mean recharge altitudes for the tunnel inflows range from 2600 to 2800 m a.s.l.

Although Figure 1 shows that a straightforward delineation of potential recharge areas is not simple due to the complex and steep topography, it is anticipated that recharge and flow through the granite body is preferentially associated to the east northeast–west southwest striking discontinuities with a strong vertical component toward the subsurface gallery. This, in turn, implies that when advancing along the tunnel profile in the southeast direction, i.e., from below the northeast-southwest trending ridge toward below the Gerental Valley bottom, the tunnel inflows are recharged from decreasing altitude zones. This trend is then reflected by the subsurface samples.

An intriguing difference from this general trend can be observed at the sampling points T9, T11, and S1. Here, more anomalously negative $\delta^{18}O$ values are observed than would otherwise be predicted by the decrease in overburden and, thus, in potential recharge altitude. The $\delta^{18}O$ depleted values may be attributed to two factors: (1) the additional component from the glacial meltwater in the ground water recharge via the fault zone to the gallery, as well as an additional altitude effect as indicated by numerical simulations of the ground water flow (Ofterdinger et al. submitted); and (2) the $\delta^{18}O$ composition of the sampled ground water in the northern part of the tunnel can be assumed to be derived by recharge from accumulated winter precipitation and actual summer precipitation during the recharge period. The ground water samples taken along the fault zone, however, show the imprint of recharge by these two components, plus the additional component of glacial ice. Even though this additional component is enriched in ^{18}O due to fractionation processes in the transition from snow to ice (Stichler and Schotterer 2000), the resulting $\delta^{18}O$ content is still isotopically lighter than actual summer precipitation. This additional glacial component will thus shift the resulting overall $\delta^{18}O$ concentration in the ground water recharge from the glaciated areas toward more negative values.

Additionally, a numerical ground water flow model of the study area (Ofterdinger et al. submitted), in which the major fault zone was included with discrete higher conductive elements, shows that recharge via the fault zone to the tunnel occurs mainly along the upper slopes of the glaciated areas between Geren- and Muttenglacier, plus to the south along the upper region of the north-facing slope of the Rotondo Summit. This higher recharge altitude, compared to the neighboring sample locations in the north of the tunnel, is also contributing to the depleted $\delta^{18}O$ values encountered along the fault zone section of the tunnel.

Figure 8 shows the temporal variations in $\delta^{18}O$ values for ground water sampled at observation point T9, as well as the mean signal from the remaining observation points. The temporal variations at the individual sampling locations are small (≤ 0.2‰; highest along the fault zone section), indicating a lack of correlation to small-scale temporal variations in $\delta^{18}O$ of precipitation.

Lumped-Parameter Model

To analyze the relationship between precipitation input and glacial meltwater in ground water recharge, the observed $\delta^{18}O$ values were introduced in a simplified transport model using a convolution/lumped-parameter approach (Maloszewski and Zuber 1996, 1998). Even though the $\delta^{18}O$ seasonal variations at the tunnel inflows show only a highly damped response (Figure 8), investigation by means of model calculations seem beneficial to assess the role of precipitation and glacial meltwater in ground water recharge.

In this investigation, we applied two approaches to reproduce the observed $\delta^{18}O$ values in ground water samples taken along the major fault zone in the tunnel. First, we introduced the precipitation input into the model to investigate whether observed $\delta^{18}O$ values in the tunnel can be reproduced solely by this precipitation-derived input function. In a second approach, we modified the precipitation input function by adding a glacial meltwater component.

The $\delta^{18}O$ input function for precipitation (1970–1999) was derived from the stations Guttannen, Meiringen, and Grimsel (1970–1999), as well as from additionally analyzed data from the stations Gütsch, Andermatt, Oberwald, Binn, and Robiei (1998–1999). The extrapolation to the mean recharge altitude of the massif above the tunnel was carried out following Equation 2 for a series of potential recharge altitudes of the massif above the tunnel, ranging from minimum elevation of 2200 m a.s.l. to maximum elevation of 3000 m a.s.l. The resulting $\delta^{18}O$ signal in precipitation shows large seasonal variations of ~14‰ with $\delta^{18}O$ values ranging from ~–6‰ during summer down to ~–20‰ during winter months. Finally, weighing of the input function by the mean monthly ground water recharge rates, derived from the hydrological model (Vitvar and Gurtz 1999), was performed.

The applied code (Maloszewski and Zuber 1996) solves the direct problem, calculating the theoretical output concentration to a given input concentration (input function) from the convolution integral for a chosen transit time distribution (parameterized by the mean residence time) under constant flow assumption. The inverse problem is solved by a trial-and-error procedure with the possibility to choose between six model types for the transit time distribution (exponential, piston-flow, linear, dispersion, exponential-piston-flow, and linear-piston-flow). The best fit between the calculated output curve and observation data is judged by an error criterion (standard deviation σ).

During the modeling process, it could be observed that, regardless of model type and model parameters, the theoretical output curves calculated from the precipitation input function showed enriched $\delta^{18}O$ values compared to the observed data. Figure 8 illustrates this behavior. This observation holds even when the extrapolation of the input function is carried out to the maximum potential recharge altitude (with the potentially maximum depleted $\delta^{18}O$ signal). This implies that the input function derived from precipitation data alone cannot explain the observed $\delta^{18}O$ depleted data. This discrepancy indicates that recharge from a $\delta^{18}O$ depleted source such as accumulated recent winter precipitation and/or glacial meltwater has a significant share in the overall recharge. Two main scenarios need to be considered to address this discrepancy.

First, recent depleted winter precipitation is accumulated and stored in the snow cover during the winter and enters the flow system in large amounts during the melting season in spring and summer, when most of the recharge to the ground water flow system occurs. As weighing of the input function is done by the calibrated recharge rates (Vitvar and Gurtz 1999), this latter observation is included in the analysis. The $\delta^{18}O$ concentrations in the input function and, thus, in recharge, are derived from precipitation. However, this precipitation-derived input function does not properly represent the input to the flow system during the melting period. Second, an additional source of depleted $\delta^{18}O$ values is present in parts of the recharge area in the form of glaciers. This additional source of depleted $\delta^{18}O$ is not accounted for in the precipitation-derived input function.

Considering these scenarios, it seems plausible to modify the input function to accommodate the $\delta^{18}O$ concentrations of the glacial meltwaters. Therefore, in a second approach, we modified the input function to the model by combining the monthly precipitation data with the glacial meltwater component. In the numerical ground water flow model (Ofterdinger et al. submitted), the ground water recharge area to the fault zone section along the tunnel (and thus to sampling point T9) was delineated through particle tracking. As previously mentioned, this recharge area comprises parts of the Geren- and Witenwasserenglacier, as well as parts of the north-facing slope of the Rotondo Summit. The calibrated hydrological model (Vitvar and Gurtz 1999) resolves apart from the monthly ground water recharge rate in this area, as well as the fraction of meltwater and actual precipitation participating in the corresponding ground water recharge. The $\delta^{18}O$ signal of the modified input function was derived by combining the $\delta^{18}O$ signal in

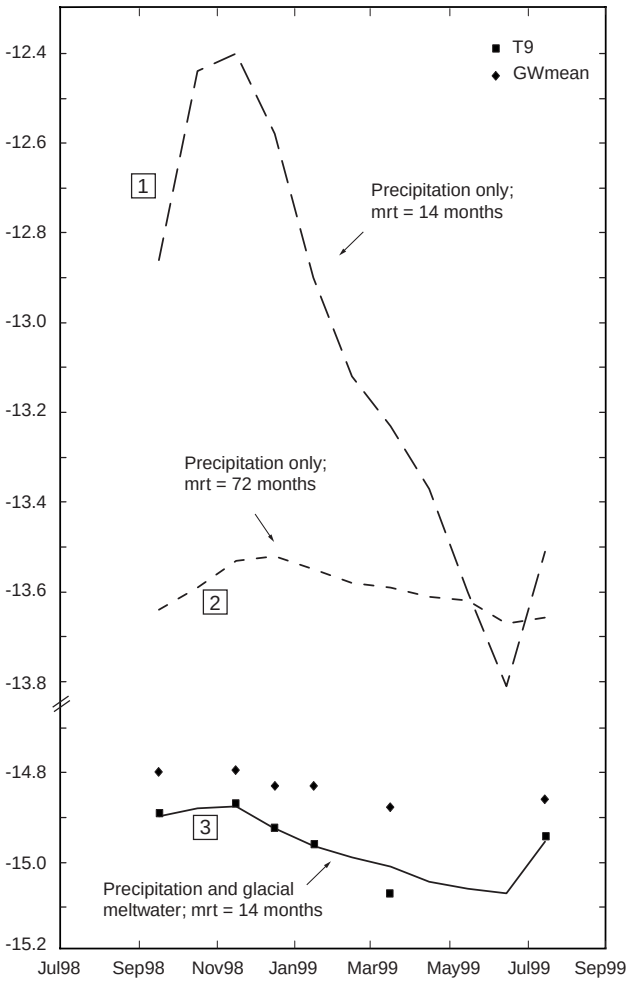

Figure 8. Observed $\delta^{18}O$ data at station T9 and calculated mean signal of remaining ground water sampling stations (GWmean). Indicated is the output function for lumped-parameter modeling representing the best fit to the observed data when the precipitation-derived input function is modified by an additional meltwater component (line 3). Line 1 illustrates the output function for solely precipitation-derived input function for identical model parameters of the best fit model. Even for potential large residence times (line 2), the output function from the precipitation-derived input function remains enriched compared to the observed data (mrt = mean residence time).

precipitation and the $\delta^{18}O$ signal in the meltwater ($c\beta$) according to their contribution to the monthly ground water recharge.

From the available model types, a best fit in terms of shape of the output function, as well as in error criterion, was achieved by applying the exponential model combined with a piston-flow component (EPM). The applied ratio of total volume to the volume with the exponential distribution of transit times, η, was 1.2. The necessity to apply a combined model in order to achieve a good fit as in this case is most probably linked to the nature of the granitic rocks. These provide, due to zones of dense fracturation and faults as well as more intact massive rock, different flow components with different transit time distributions. As the modeled $\delta^{18}O$ signal (sampling location T9) is associated with the major fault zone with dense fracturation, it is not surprising that a combined model leads to the best fit.

The best fit of the EPM model to the observed $\delta^{18}O$ data (Figure 8) yields a mean residence time of ~14 months with an error criterion of $\sigma = 0.0096‰$. The lack of strong variations in the observed $\delta^{18}O$ signal in the ground water, despite the short residence time, is mainly attributable to the large fraction of glacial meltwater contributing to the ground water recharge (~70% of annual recharge) compared to liquid summer precipitation.

Discussion and Conclusions

Several approaches have been shown to give information on the origin of the ground water encountered in the Rotondo Granite and especially on the conditions of recharge, in particular, the influence of the glaciated regions in the study area. While the interpretations of the individual investigated parameters offer potential answers to the previous questions, a more compelling scenario can be deduced by combining the results of the individual investigation.

In general, all investigated parameters show that, at the tunnel elevation, only little temporal variations can be observed. The measured $\delta^{2}H/\delta^{18}O$ signal in ground water shows its meteoric origin (Figure 6). Hydrochemical analysis of the tunnel inflows shows that their composition can be explained as an evolution along the flowpath within the granite body. Flow is hereby assumed to be preferentially orientated along the steeply dipping fractures and faults, following an overall east northeast–west southwest strike.

Tritium, temperature, and $\delta^{18}O$ content measured along the tunnel profile (Figure 4) all show anomalous behavior below the glaciated areas. As this section is at the same time situated approximately below the valley bottom, two potential explanations for these observations need to be addressed.

Contribution of old ground water components upwelling below the valley bottom may be associated with low tritium content. This would be in agreement with the observation. The tritium/sodium correlation observed is no compelling indicator for the contribution of older ground water components because sodium concentrations are still very small and the correlation is most probably only a spatial coincidence and no causal relationship. The conductivity measurements and hydrochemical analysis of the ground water give also no evidence of old ground water components with potentially higher mineralization. Furthermore, the negative temperature anomaly is not explained by this scenario.

A second explanation for the observed data would be a significant contribution of cold submodern glacial meltwater from the overlaying glaciers with low tritium concentrations and depleted $\delta^{18}O$ values. Model calculations underline the contribution of this $\delta^{18}O$ depleted source to ground water recharge and even though the absolute figures of this model should be treated with care because of the simplified model assumption, the significance of this contribution is demonstrated. The large fault zone associated with the inflows where this anomaly is observed is hereby providing a preferential flowpath. Due to the subvertical east northeast–west southwest strike of this structure, a potentially large glaciated area with topographic elevation up to 3000 m a.s.l. (Figure 1) is tapped. Ground water recharged along the strike of this structure in the glaciated areas is believed to move by topography-driven flow and enhanced by drainage to the subsurface gallery along this preferential flowpath toward the tunnel, whereby preserving the glacial signature.

On the whole, these investigations suggest that the ground water flow system within the Rotondo Granite is recharged by meteoric waters with significant contribution of glacial meltwater, as well as meltwater from accumulated recent winter precipitation. Recharge contributions from the glaciated areas is therefore enhanced by the orientation of the water-conducting fracture sets and fault zones.

Temporal variations in the observed parameters of the ground water are small. Cross flow from neighboring formations is minor and is, if at all present, mainly restricted to the northern boundary of the granite body. The ground water becomes moderately mineralized along the flowpath within the granite, mainly through the process of silicate weathering (plagioclase hydrolysis). Model calculations approximate the mean residence times of the encountered ground water along the fault zone section in the gallery of ~1 to 1.5 yr and underline the significant contribution of glacial meltwater to ground water recharge. Even though the absolute figure of the mean residence time should be regarded as an approximation due to the involved simplifications, it indicates rather rapid recharge from the glaciated areas via the fault zone to the gallery.

In general, the findings of this study indicate that in a high alpine catchment, accumulated winter precipitation and glacial meltwater may contribute significantly to recharge of deep ground water flow systems. Permeable fault zones may therefore yield preferential pathways for rapid recharge from these components to deep ground water flow systems.

Acknowledgments

Precipitation samples from the meteorological stations at Gütsch, Andermatt, Oberwald, Binn, and Robiei were kindly taken by the station supervisors. Data from the stations Guttannen, Meiringen, and Grimsel were obtained from the Schweizerische Meteorologische Anstalt-SMA, Zürich and the Landeshydrologie, Bern, as well as

extracted from the Global Network for Isotopes in Precipitation database provided by the International Atomic Energy Agency, Vienna. Access to the Furka Basetunnel and the Bedretto Tunnel, as well as logistic help, was kindly provided by the Furka-Oberalp-Bahn. This research was funded by the ETH research fund. The authors also express their thanks to Ian Clark, C.K. Keller, and an anonymous reviewer for helpful reviews of the manuscript.

References

Abbott, M., A. Lini, and P. Bierman. 2000. $\delta^{18}O$ and ^{3}H measurements constrain groundwater recharge patterns in an upland fractured bedrock aquifer, Vermont, USA. *Journal of Hydrology* 228, 101–112.

Ambach, W., H. Eisner, R. Haefeli, and M. Zobl. 1971. Bestimmung von Firnrücklagen am Eisschild Jungfraujoch durch Messung der Gesamtbetaaktivität von Firnproben. *Zeitschrift für Gletscherkunde und Glazialgeologie* 7, 57–62.

Ambach, W., H. Eisner, H. Moser, W. Rauert, and W. Stichler. 1971. Ergebnisse von Isotopenmessungen am Gletscherbach des Kesselwanferners (Ötztaler Alpen). *Annalen der Meteorologie* 5, 209–218.

Arnold, A. 1970. On the history of the Gotthard-massif (Central Alps, Switzerland). *Eclogae Geologicae Helvetiae* 63, 29–30.

Ball, J.W., and D.K. Nordstrom. 1992. User's manual for WATEQ4F, with revised thermodynamic data base and test cases for calculating speciation of major, trace, and redox elements in natural waters. U.S. Geological Survey Technical Open-File Report 91–183.

Clark, I.D., and P. Fritz. 1997. *Environmental Isotopes in Hydrogeology*. Boca Raton, Florida: Lewis Publishers.

Craig, H. 1961. Isotopic variations in meteoric waters. *Science* 133, 1702–1703.

Cruchet, M. 1985. Influence de la decompression sur le comportement hydrogeologique des massifs cristallins en basse Maurienne (Savoie, France). *Géologie Alpine* 61, 65–73.

Dubois, J.-D. 1993. Typologie des aquifères du cristallin: Exemple des Massifs des Aiguilles Rouges et Du Mont-Blanc (France, Italie et Suisse). Ph.D. thesis, Département de Génie Civil, GEOLEP, Ecole polytechnique fédérale de Lausanne, France.

Flerchinger, G.N., K.R. Cooley, and D.R. Ralston. 1992. Groundwater response to snowmelt in a mountainous watershed. *Journal of Hydology* 133, 293–311.

Fontes, J.-C., G.C. Bortolami, and G.M. Zuppi. 1978. Hydrologie isotopique du massif du Mont Blanc. In *Proceedings of Symposium, Isotope Hydrology*, June 19–23, Neuherberg, vol. 1, 411–440. Vienna: International Atomic Energy Agency.

Forster, C., and L. Smith. 1988a. Groundwater flow systems in mountainous terrain, 1. Numerical modeling technique. *Water Resources Research* 24, no. 7: 999–1010.

Forster, C., and L. Smith. 1988b. Groundwater flow systems in mountainous terrain, 2. Controlling factors. *Water Resources Research* 24, no. 7: 1011–1023.

Gat, J. 1981. Groundwater. In *Stable Isotope Hydrology: Deuterium and Oxygen-18 in the Water Cycle*, IAEA Technical Report Series No. 210, ed. J. Gat and R. Gonfiantini, 223–240.

Gat, J. 2000. Atmospheric water balance—The isotopic perspective. *Hydrological Processes* 14, 1357–1369.

Hafner, S. 1958. Petrographie des südwestlichen Gotthardmassivs. *Schweizerische Mineralogische und Petrographische Mitteilungen* 38, 255–362.

Hoefs, J. 1997. *Stable Isotope Geochemistry*. Berlin: Springer.

ISO. 1997. Measurement of liquid flow in open channels—Velocity-area methods. International Organization for Standardization Technical Report ISO 748: 1997(E).

ISO. 1980. Water flow measurements in open channel using weirs and venturi flumes, Part 1. Thin-plate weirs. International Organization for Standardization Technical Report ISO 1438/1–1980(E).

Jäger, E., and E. Niggli. 1964. Rubidium-Strontium-Isotopenanalysen an Mineralien und Gesteinen des Rotondogranits und ihre geologische Interpretation. *Schweizerische Mineralogische und Petrographische Mitteilungen* 44, no. 1: 61–81.

Jouzel, J., and L. Merlivat. 1984. Deuterium and oxygen 18 in precipitation: Modeling of the isotopic effects during snow formation. *Journal of Geophysical Research* 89, no. D7: 11749–11757.

Kattelmann, R., and K. Elder. 1991. Hydrologic characteristics and water balance of an alpine basin in the Sierra Nevada. *Water Resources Research* 27, no. 7: 1553–1562.

Keppler, A. 1996. Hydrogeologische, hydrochemische und isotopenhydrologische Untersuchungen an den Oberflächen- und Kluftwässern im Grimselgebiet, Schweiz. GSF-Bericht 4/96. Neuherberg: GSF-Forschungszentrum für Umwelt und Gesundheit.

Lhomme, D., M. Dzikowski, G. Nicoud, B. Payraud, S. Fudral, and P.-L. Guillot. 1996. Les circulations actives des eaux souterraines des massifs cristallins alpins: Exemple des Aiguilles Rouges (Haute-Savoie, France). *Compte rendu Académie des Sciences (série IIa)* 323, 681–688.

López, D.L., and L. Smith. 1995. Fluid flow in fault zones: Analysis of the interplay of convective circulation and topographically driven groundwater flow. *Water Resources Research* 31, no. 6: 1489–1503.

Malard, F., K. Tockner, and J. Ward. 1999. Shifting dominance of subcatchment water sources and flow paths in a glacial floodplain, Val Roseg, Switzerland. *Arctic, Antarctic and Alpine Research* 31, no. 2: 135–150.

Maloszewski, P., and A. Zuber. 1996. Manual on mathematical models in isotope hydrology. International Atomic Energy Agency Technical Report TECDOC–910.

Maloszewski, P., and A. Zuber. 1998. A general lumped parameter model for the interpretation of tracer data and transit time calculation in hydrologic systems: Comments. *Journal of Hydrology* 204, 297–300.

Marechal, J.-C. 1998. Les circulations d'eau dans les massifs cristallins alpins et leurs relations avec les ouvrages souterrains. Ph.D. thesis, Département de Génie Civil, GEOLEP, Ecole polytechnique fédérale de Lausanne, France.

Martinec, J., H. Oeschger, U. Schotterer, and U. Siegenthaler. 1982. Snowmelt and groundwater storage in an alpine basin. In *Hydrological Aspects of Alpine and High Mountain Areas*, 169–175. Wallingford, United Kingdom: IAHS Press.

Ofterdinger, U.S., P. Renard, and S. Loew. Submitted. Numerical modeling of the ground water flow systems in the Rotondo Granite. *Hydrogeology Journal.*

Pearson, F., W. Balderer, H. Loosli, B. Lehmann, A. Matter, T. Peters, H. Schmassmann, and A. Gautschi. 1991. Applied isotope hydrogeology—A case study in northern Switzerland. National Cooperative for the Disposal of Radioactive Waste Technical Report 88–01.

Pistre, S. 1993. Rôle de la fracturation dans las circulations souterraines du massif granitique de Millas (Pyrénées-Orientales). *Compte rendu Académie des Sciences (série II)* 317, 1417–1424.

Priest, S.D. 1993. *Discontinuity Analysis for Rock Engineering*. London: Chapman and Hall.

Rodhe, A. 1998. Snowmelt-dominated systems. In *Isotope Tracers in Catchment Hydrology*, ed. C. Kendall and J.J. McDonnell, 391–433. Amsterdam: Elsevier.

Schotterer, U., T. Stocker, J. Hunziker, P. Buttet, and J.-P. Tripet. 1995. Isotope im Wasserkreislauf—Ein neues eidgenössisches Messnetz. *Gas Wasser Abwasser* 9, 1–8. Sonderdruck Nr. 1348 des Schweizerischen Vereins des Gas- und Wasser faches (SVGW), Zürich.

Stichler, W., and U. Schotterer. 2000. From accumulation to discharge: Modification of stable isotopes during glacial and post-glacial processes. *Hydrological Processes* 14, 1423–1438.

Tóth, J. 1963. A theoretical analysis of groundwater flow in small drainage basins. *Journal of Geophysical Research* 68, no. 16: 4795–4812.

Tóth, J. 1984. The role of regional gravity flow in the chemical and thermal evolution of ground water. In *Proceedings of the First Canadian/American Conference on Hydrogeology: Practical Applications of Ground Water Geochemistry*, June 22-26, Banff, Alberta, Canada, ed. B. Hitchon and E. Wallick, 3–39. Worthington, Ohio: National Water Well Association.

Tranter, M., G.H. Brown, A.J. Hodson, and A.M. Gurnell. 1996. Hydrochemistry as an indicator of subglacial drainage system structure: A comparison of alpine and sub-polar environments. *Hydrological Processes* 10, 541–556.

Vitvar, T., and J. Gurtz. 1999. Spatially distributed hydrological modeling in the Rotondo area, western Gothard-Massif. Technical Report 3465/16, ETH-Zürich, Engineering Geology, ETH-Hönggerberg.

Ward, J., F. Malard, K. Tockner, and U. Uehlinger. 1999. Influence of ground water on surface water conditions in a glacial flood plain of the Swiss Alps. *Hydrological Processes* 13, 277–293.

Zijl, W. 1999. Scale aspects of groundwater flow and transport systems. *Hydrogeology Journal* 7, 139–150.